High Energy Physics and Nuclear Physics

Volume 13, No. 1

Relativistic Study of Proton-Nucleus Elastic Scattering at Lower Energies

Li Yangguo

(Department of Physics, Shantou University, Guang Dong)

The Lorentz invariant relativistic optical potential has been discussed at energies below 300 MeV. The Dirac equation with scalar and vector potentials is exactly solved by the partial wave method. The calculated results of proton-^{40}Ca in the energy region 300-65 MeV are presented and compared with the experimental data of the differential cross section $d\sigma/d\Omega$, analyzing power $A_y(\theta)$ and spin rotation function $Q(\theta)$. It can be shown that the improved relativistic optical potential fits data well.

1. INTRODUCTION

Since the early 1980's, great successes on relativistic studies of the proton-nucleus interaction have been achieved [1,2]. In the field of elastic scattering, problems studied have been focused on characteristics of the relativistic optical potential. By solving the Dirac equation, in which the optical potential is included, phenomenologically or microscopically [3,4], the experimental data, the differential cross section $d\sigma/d\Omega$, the analyzing power of the spin observable $A_y(\theta)$, and the spin rotation function $Q(\theta)$, can be well described. These three quantities are mutually independent and form a set of complete measure. The above theoretical studies were mainly developed with the inspiration from the meson exchange theory of the nuclear force proposed in recent years. With the Lorentz invariant N-N scattering amplitudes, the optical potential in the Dirac equation in the medium energy region could be derived in terms of the relativistic self-consistent field theory. In this optical potential, all possible terms in the Lorentz transformation are included, and, at least, two of

Supported by the National Natural Science Foundation of China.
Received on December 19. 1987.

them, i.e. the scaler term S and the vector term V, are of equal importance in quantity. As a result, convincing successes have been achieved in the higher energy region where the energy of the incident proton, T_p, is greater than 500 MeV.

However, in the lower energy region where the energy of the incident proton is less than 300 MeV, it is difficult to explain the experimental data by using the optical potential in the relativistic impulse approximation, because the scalar term S and the vector term V in this potential are too Strong [5,6]. Tjon [6] modified the optical potential by using the meson exchange theory and obtained primarily a better result. In this paper, we further improve Tjon's potential and study p + ^{40}Ca scattering in the energy region between 65 MeV and 300 MeV. As a consequence, we obtain a better agreement between the theoretical result and the experimental data.

2. MODIFICATION OF THE RELATIVISTIC OPTICAL POTENTIAL

The multi-scattering theory [2,3,4] has been developed by studying the relativistic proton-nucleus elastic scattering. With this theory, the Dirac optical potential, U_{opt}, has been derived. This potential is the Lorentz invariant and has the following form:

$$U_{opt} = S(\boldsymbol{r}) + \gamma^{\mu} V_{\mu}(\boldsymbol{r}) + \sigma^{\mu\nu} T_{\mu\nu}(\boldsymbol{r}) + \gamma^5 P(\boldsymbol{r}) + \gamma^5 \gamma^{\mu} A_{\mu}(\boldsymbol{r}), \tag{1}$$

where $S(\boldsymbol{r})$, $\gamma^{\mu} V_{\mu}(\boldsymbol{r})$, $\sigma^{\mu\nu} T_{\mu\nu}(\boldsymbol{r})$, $\gamma^5 P(\boldsymbol{r})$, and $\gamma^5 \gamma^{\mu} A_{\mu}(\boldsymbol{r})$ are the scalar, vector, tensor, pseudoscalar, and pseudovector potentials, respectively, and $\sigma^{\mu\nu}$ and γ are 4 × 4 matrices in Bjorken's definition, respectively. The pseudoscalar and pseudovector potentials do not contribute to U_{opt}, because of the parity conservation, while the tensor potential has only 1% contribution to U_{opt}, so it can be neglected [4]. By adopting this optical potential, one can successfully explain the experimental data of spin observables in the energy region of above 500 MeV, but not properly reproduced the experimental data in the energy region of below 300 MeV, because of the overstrong $S(r)$ and $V(r)$ in the latter case [5,6] and other reasons. Therefore, Tjon[6] proposed a generalized relativistic impulse approximation method, namely, to consider the NN interaction in the whole Dirac spinor space and use the generally accepted pseudovector π-meson exchange instead of the pseudoscalar single π-meson exchange. After considering the parity conservation, the time-reversal invariance, and the charge symmetry, one can obtain the optical potential in a more completed form

$$\begin{aligned} U_{opt} = {} & S(r) + \gamma^0 V(r) + C(r) \left[\frac{-E\gamma^0 + \boldsymbol{\gamma} \cdot \boldsymbol{p} + m}{m} \right] - i\boldsymbol{\alpha} \cdot \boldsymbol{\gamma} T(r) \\ & - \{ S_{LS}(r) + \gamma^0 V_{SL}(r) \} \boldsymbol{\sigma} \cdot \boldsymbol{L} - i\boldsymbol{\gamma} \cdot \boldsymbol{r} D(r) + F(r) \boldsymbol{\alpha} \cdot \boldsymbol{p}, \end{aligned} \tag{2}$$

where the last two terms comes from the off-shell effect of the NN amplitude. If one uses the on-shell NN amplitudes, the last two terms vanish. The strengths of $T(r)$ $S_{LS}(r)$, and $V_{SL}(r)$ are about 1 MeV. They are much smaller than those of the first three terms and thus can be neglected. Finally, one can take the sum of the first three terms as the relativistic optical potential

$$U_{opt} = S(r) + \gamma^0 V(r) + C(r) \left[\frac{-E\gamma^0 + \boldsymbol{\gamma} \cdot \boldsymbol{p} + m}{m} \right] \tag{3}$$

Substituting Eq.(3) into the Dirac equation [4], and inserting a factor $(1 + C(r)/m)$ into the

wave function one obtains the equivalent Dirac equation

$$\{\boldsymbol{\alpha}\cdot\boldsymbol{p}+\beta[m+\tilde{S}(r)]+\tilde{V}(r)+\tilde{V}_c(r)\}\tilde{\psi}_k^{(+)}(\boldsymbol{r})=E\tilde{\psi}_k^{(+)}(\boldsymbol{r}), \tag{4}$$

where the corresponding scalar, vector, and coulomb potentials are

$$\left.\begin{aligned}\tilde{S}(r)&=S(r)\Big/\left[1+\frac{C(r)}{m}\right],\\ \tilde{V}(r)&=V(r)\Big/\left[1+\frac{C(r)}{m}\right],\\ \tilde{V}_c(r)&=V_c(r)\Big/\left[1+\frac{C(r)}{m}\right].\end{aligned}\right\} \tag{4.1}$$

It is clear that, due to the consideration of the pseudovector πN exchange, the strengths of $\tilde{S}(r)$ and $\tilde{V}(r)$ change greatly at the energy below 300 MeV. For instance, when T_p is 100 MeV, the results are less than half of those obtained with the pseudoscalar πN exchange. These strengths are slowly increasing with decreasing T_p. From this relativistic theory, one further knows that $V(r)$ and $S(r)$ have very strong strengths and opposite signs. The relativistic result depends very much on the shapes of these potentials, which correspond to the density distributions of the scalar and vector potentials [4]. In order to study the validity of the relativistic theory in the lower energy region, examine the effect of the improvement, and reveal the existing problems, we choose the Saxon-Woods form for potentials in Eq. (4), and exactly solve the Dirac equation.

3. CALCULATIONS OF OPTICAL POTENTIALS IN THE DIRAC EQUATION

In order to obtain $d\sigma/d\Omega$, $A_y(\theta)$ and $Q(\theta)$ in the proton-nucleus elastic scattering process, the relativistic optical potential described in Eq.(4) is employed and the Dirac equation is exactly solved by using the partial wave method in the coordinate space. The strengths of $S(r)$ and $V(r)$ are chosen to be those in Ref. [6], and the shapes of these potentials are taken in the Saxon-Woods form

$$\left.\begin{aligned}\tilde{S}(r)&=V_s f_s(r)+iW_s f_{ws}(r),\\ \tilde{V}(r)&=V_0 f_0(r)+iW_0 f_{w0}(r).\end{aligned}\right\} \tag{5}$$

and

$$f_i(r)=\frac{1}{1+e^{(r-R_i)/a_i}}. \qquad (i=s, ws, 0, w0) \tag{6}$$

The coulomb potential $\tilde{V}_c(r)$ is chosen according to the homogenous charge distribution [4]. In this optical potential, 12 parameters at most are required. Compared with the nonrelativistic description in which 12 parameters are required to describe the optical potential including the spin-orbit term, this means that the number of parameters in the relativistic description is not increased. The parameters of shapes of all nuclear optical potentials at T_p = 500 MeV have been given in Ref. [4]. By starting with these values and referring to our or others'[8] findings that small changes of shapes of optical potentials, i.e., small changes of the nuclear density distribution, would greatly affect the values of spin observable, such as $A_y(\theta)$ and $Q(\theta)$, these parameters can be further adjusted until

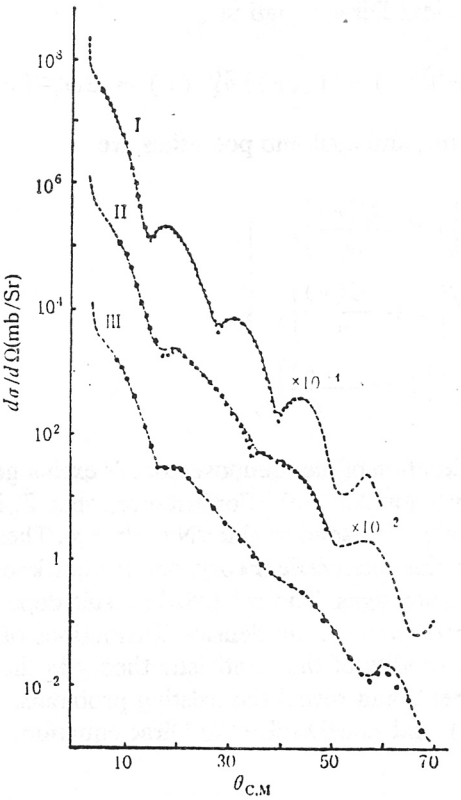

FIGURE 1 The scattering differential cross section of p + ^{40}Ca, Energy I: 300 MeV; II: 200 MeV; III: 181.7 MeV. Dots are the experimental data.

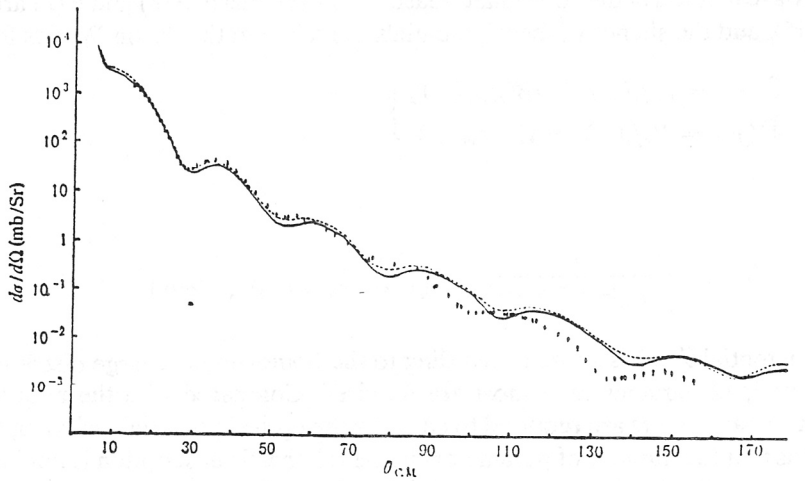

FIGURE 2 The scattering differential cross section of p + ^{40}Ca at T_p = 65 MeV. Dots are the experimental data, the solid and dashed curves are theoretical results with parameter sets III and I, respectively.

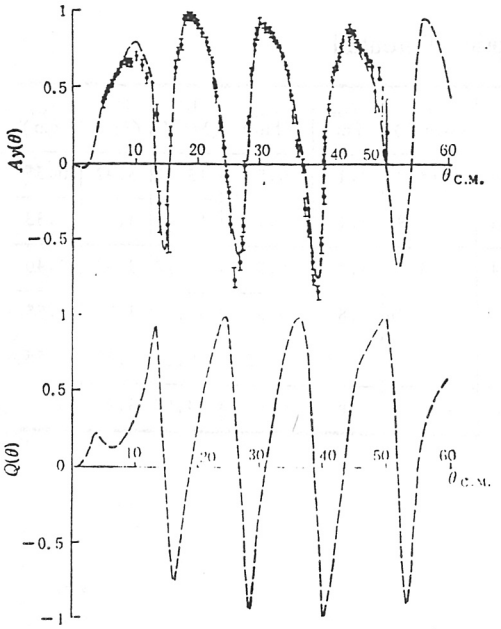

FIGURE 3 The analyzing power $A_y(\theta)$ and the spin rotation function $Q(\theta)$ of p + ^{40}Ca at T_p = 300 MeV. Dots are the experimental data and the curves are theoretical results.

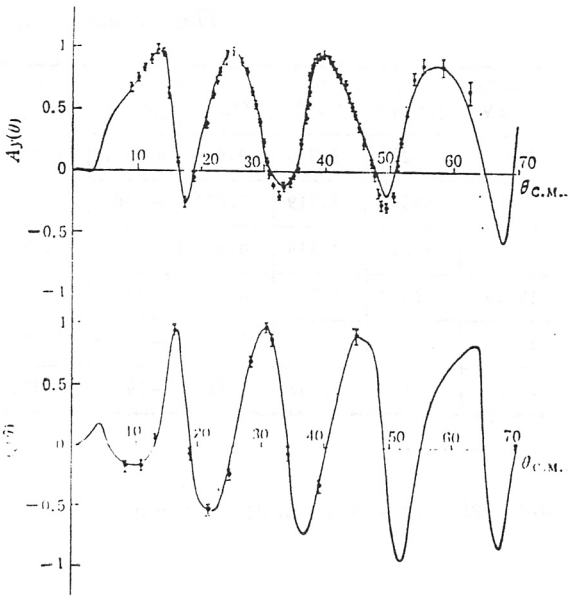

FIGURE 4 Same as Fig.3, except T_p = 200 MeV.

the experimental data are better reproduced. In practical calculation, it is rather difficult to optimize the values of the multitude of parameters, even with an automatic search program. In order to overcome this difficulty, the sieve method was repeatedly used until the best result is obtained. In this method, all variables are divided into several groups and two to three variables containing in one group, are varied each time.

The reduction of the Dirac equation has been discussed in Ref. [4]. After calculating the amplitudes of the spin normal term $F_1(\theta)$ and the spin flip term $F_2(\theta)$, the scattering amplitude can be written as

$$M(\theta) = F_1(\theta) + \boldsymbol{\sigma} \cdot \boldsymbol{n} F_2(\theta), \tag{7}$$

where $\boldsymbol{\sigma}$ is the Pauli matrix for the incident proton, and $\hat{n} = \hat{k}_i \times \hat{k}_f$ is the unit vector perpendicular to the scattering plane. Consequently, the differential cross section can be expressed as

$$\frac{d\sigma}{d\Omega} = |F_1(\theta)|^2 + |F_2(\theta)|^2, \tag{8}$$

TABLE 1
The Parameters of the Optical Potential

energy (MeV)	V_0 (MeV)	R_0 (fm)	a_0 (fm)	V_s (MeV)	R_s (fm)	a_s (fm)	W'_0 (MeV)	R_{w0} (fm)	a_{w0} (fm)	W'_s (MeV)	R_{ws} (fm)	a_{ws} (fm)
65 I	362.	3.519	0.637	−450.	3.488	0.664	−18.9	4.1	0.5	13.78	3.42	0.35
II	362.	3.519	0.637	−450.	3.488	0.664	−18.9	4.1	0.5	13.78	3.42	0.33
III	362.5	3.519	0.637	−454.1	3.488	0.664	−18.9	4.1	0.5	13.78	3.42	0.40
181.3	320.9	3.587	0.618	−439.2	3.556	0.646	−71.36	3.8	0.6	55.92	3.76	0.55
200.	301.9	3.587	0.618	−406.8	3.556	0.646	−74.3	3.83	0.623	69.27	3.83	0.58
300.	281.2	3.587	0.618	−399.9	3.556	0.646	−83.6	3.9	0.615	84.57	3.9	0.6

the analyzing power can be written as

$$A_y(\theta) = \frac{2\mathrm{Re}(F_1(\theta)F_2^*(\theta))}{|F_1(\theta)|^2 + |F_2(\theta)|^2}, \tag{9}$$

and the spin rotation function can be calculated by

$$Q(\theta) = \frac{2\mathrm{Im}(F_1(\theta)F_2^*(\theta))}{|F_1(\theta)|^2 + |F_2(\theta)|^2}, \tag{10}$$

The calculated results, which are the best results at the present moment, for the p + ^{40}Ca system in the energy region from 65 MeV to 300 MeV are plotted in Figs.1-6. The experimental data [5,9] are also plotted in these figures. The parameters of optical potentials for the theoretical

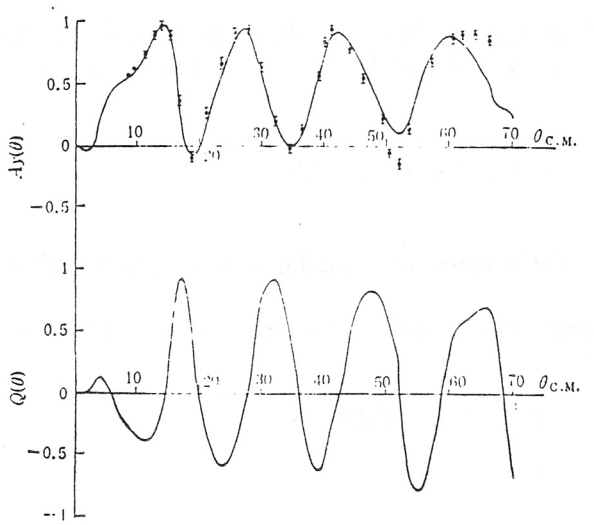

FIGURE 5 Same as Fig.3, except T_p = 181.7 MeV.

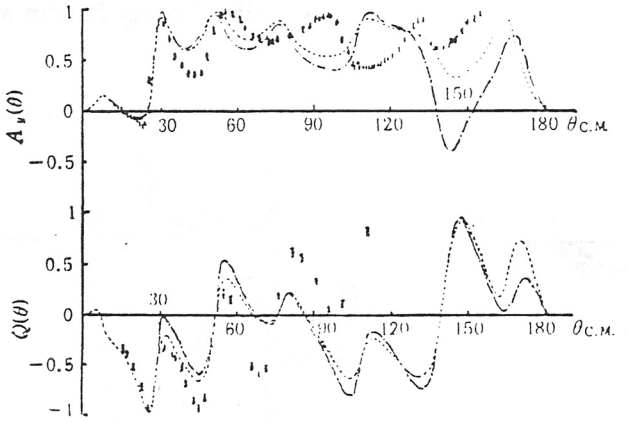

FIGURE 6 Same as Fig.3, except T_p = 65 MeV. The dashed and dot-dashed curves are results with parameter sets III and I, respectively.

calculation are tabulated in Table 1. In the case of T_p = 65 MeV, the computation is performed in the angular region from 0° to 180°.

4. ANALYSIS AND DISCUSSION

From these figures, one can see that in the cases of T_p = 300, 700, and 181.3 MeV, very good agreements between the calculated $d\sigma/d\Omega$, $A_y(\theta)$, and $Q(\theta)$ and the experimental data in the experimental angular region are obtained. Compared with the results obtained in the relativistic impulse approximation, such as the results published by Hynes and Cleak et al. [5], and those obtained by using the non-relativistic optical potential, our result looks better. At T_p = 200 MeV, it is very similar to that given by Wallace [6] at the Beijing International Symposium on Medium Energy Physics. At lower energy, T_p = 65 MeV, since the experimental data published by Sakagochi et al. [9] recently span over a wide angular range, we give the result in the whole angular region. At angles smaller than 90°, the differential cross section almost coincides with the experimental data. At angles larger than 90°, the deviation of the theoretical $d\sigma/d\Omega$ from the experimental data is not too large and the calculated positions of peaks and dips of $d\sigma/d\Omega$ curves are quite close to the experimental ones. The calculated analyzing power $A_y(\theta)$ and spin rotation function $Q(\theta)$ coincide with the experimental data at angles smaller than 30°, almost fit the experimental data at angles smaller than 60°, but only give the general features for angles larger than 90°. This indicates that the theory should be further improved. Ma et al. [10] studied this problem at the same energy by using the relativistic optical potential derived from the σ and ω meson fields. Their result is much worse than ours. Their theoretical differential cross section has a large deviation at angles larger than 50° and differs by an order of magnitude at angles larger than 90°. In comparison, the deviation in our case is within a factor of 2. The same situation holds for their calculated $A_y(\theta)$ and $Q(\theta)$. Moreover, in the non-relativistic optical potential model including the spin-orbit interaction term, there are 12 adjustable parameters. By using this potential, one is still unable to explain the behavior in the larger angle region. In order to generally describe the experimental data, one has to introduce artificially an angular momentum l related potential, such as $-V_{ex}(-1)^l f(r_{ex})$, where $f(r_{ex})$ is a potential shape function. Thus, one has to employ, at least, three more adjustable parameters.

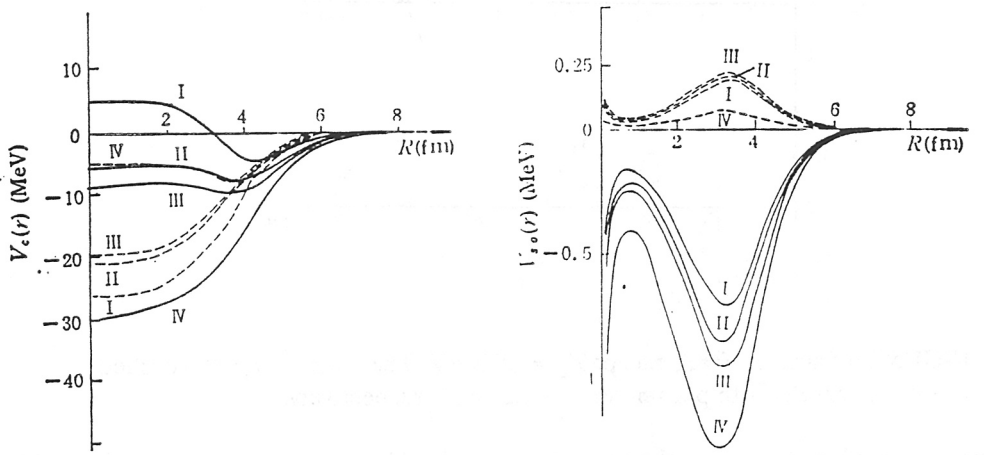

FIGURE 7 $V_c(r)$ and $V_{so}(r)$ of the elastic scattering of p + ^{40}Ca, the solid and dashed curves represent the real and imaginary parts of these potentials, I, II, III and IV denote the energies of the proton are 300, 200, 200, 181.7, and 65 MeV, respectively.

It should be pointed out that although we have obtained a rather satisfactory S-V optical potential, the spin dependent observable are still very sensitive to the change of the optical potential. At T_p = 65 MeV, we give three sets of the calculated results in Table 1. From this table, one can see that tiny changes on optical potentials cause large deviations on $A_y(\theta)$ and $Q(\theta)$. Especially, in the larger angular region, these deviations become even larger. This is very similar to Hynes' [8] analysis and his quantitative relation between the deviations and changes of the potential strengths, the density distribution, etc.. This is helpful for deeper understanding the behavior of the nucleon in the nucleus.

The calculated central potential and the real and imaginary parts of the spin-orbit potential at several energies are plotted in Fig. 7. Together with the result [3] in higher energy region, one finds that these potentials change smoothly with respect to the energy in the whole energy region (50 MeV $\leq T_p \leq$ 1000 MeV). Wallace has pointed out that at energy above 500 MeV, the improved result is very close to that obtained by using the relativistic impulse approximation in earlier days. These indicate that the pseudovector π meson exchange model is necessary in the lower energy region. Furthermore, at energies between 200 to 300 MeV, the attractive central potential becomes repulsive. This relativistic result is similar to that obtained from earlier phase shift analysis. From Table 1, one can clearly see that $S(r)$ and $V(r)$ are both strong but with opposite signs, consequently, the central potential is weak and the spin interaction is very strong. It should be mentioned that in Table 1, the parameters of the optical potential at energies above 181MeV are quite different from those given by Kobos [5]. Since there were no experimental data of the spin rotation function for ^{40}Ca to compare with at that time, their parameters of the optical potential in different sets as well as their results for spin observable are quite different.

From the above analyses, one can see that the generalized S-V Dirac optical potential in the relativistic impulse approximation is a rather successful potential. At energies above 100 MeV, the relativistic description is always better than the nonrelativistic one. At energies below 100 MeV, the result is still satisfactory. It should be further mentioned that some other phenomena would affect the nuclear scattering result. For instance, the Pauli blocking effect and the other nuclear matter

correction become more important in the lower energy region. The impulse approximation is not a good one in the lower energy and larger angular region.

REFERENCES

[1] M. R. Anastasio, L. S. Celenza, W. S. Pong and Shakin, *Phys. Report*, 100(1983)327.

[2] J. A. McNeil, J. Shepard and S. J. Wallace, *Phys. Rev. Lett.* 50(1983)1439, 1443; Qiou Xijung, et al., *Chinese Science*, A(1986)378, and its references.

[3] B. C. Clark et al., *Phys. Lett.* 122B(1983)211; *Phys. Rev. Lett.* 50(1983)1644 and Private communication; E. Rost, et al., *Phys. Rev.* C35(1987)2236; B. Aas et al., Phys. Rev. C32(1985)231.

[4] Liu Yan and Li Yangguo, *High Energy Physics & Nuclear Physics*, 11(1987)68.
Li Yangguo, *High Energy Phys. & Nucl. Phys.* 11(1987)208.

[5] B. C. Clark, et al., *Phys. Rev.* C28(1983)1421; M. V. Hynes, et al. *Phys. Rev. Lett.* 52(1984)978; A. M. Kobos, et al. *Nucl. Phys.* A445(1985)605.

[6] A. J. Tjon and S. J. Wallace, *Phys. Rev.* C32(1985)267; S. J. Wallace 'Relativistic Multiple Scattering' in International Symposium on Medium Energy Physics, June (1987).

[7] J. D. Bjorken and S. D. Drell., Relativistic Quantum Mechanics (New York 1964).

[8] M. V. Hynes, et al., *Phys. Rev.* C31(1985)1438.

[9] L. G. Arnold et al., *Phys. Rev.* C23(1981)1949; E. Steyenson, Proceedings of 'Dirac Approaches to Nuclear Physics' Los Alamos (1985); H. Sakaguchi et al., *J. Phys. Soc. Jpn. Suppl.*, 55(1986)61 and private communication.

[10] Ma Zhongyu, *High Energy Physics & Nuclear Physics* 12(1988)635.